Int. J. Cancer: **119,** 139–145 (2006)

Optical diagnosis of cervical cancer by fluorescence spectroscopy technique

Siddappa M. Chidananda[1], Kapaettu Satyamoorthy[1], Lavanya Rai[2], Attibele P. Manjunath[2] and Vasudevan B. Kartha[3]*

[1]*Center for Molecular and Cellular Biology, Manipal Academy of Higher Education, Science Center, Manipal. Karnataka, India*
[2]*Department of Obstetrics and Gynecology, Kasturba Medical College, Manipal. Karnataka, India*
[3]*Center for Laser Spectroscopy, Manipal Academy of Higher Education, Science Center, Manipal. Karnataka, India*

In the present work, we examine normal and malignant stage IIIB cervical tissue by laser induced fluorescence, with 2 different objectives. (*i*) Development of the fluorescence spectroscopy technique as a standard optical method for discrimination of normal and malignant tissue samples and, (*ii*) Optimization of the technique by the method of matching of a sample spectrum with calibration sets of spectra of pathologically certified samples. Laser-induced fluorescence spectra were measured using samples from 62 subjects at different excitation wavelengths. Principal component analysis (PCA) of spectra and intensity ratios of curve-resolved fluorescence peaks were tested for discrimination. It was found that PCA of total fluorescence at 325 nm excitation gives specificity and sensitivity over 95%. Use of calibration sets of spectra of histo-pathologically certified samples combined with PCA for matching and pass/fail classification of test samples is shown to have high sensitivity/specificity for routine diagnostic purposes as well as for possible staging of the disease. Further, the multi-component origin of the fluorescence spectra is illustrated by curve resolution and fluorescence spectra of separated proteins of tissue homogenates.

Key words: laser induced fluorescence; optical diagnosis; principal component analysis

Cervical Cancer is the second leading cancer in females all over the world, standing first in many of the developing countries.[1,2] Most patients are diagnosed with cervical cancer through symptoms such as abnormal vaginal bleeding and vaginal discharge. Investigation by Pap smear/colposcopy followed by histopathology confirms the diagnosis. Pap smear is reported to have high false negative (15–40%) rates.[3,4] The extraordinary monotony of the work, large volume of smears in screening applications, inadequate sampling and comparatively smaller cellular changes being overlooked because of fatigue are all reasons ascribed to the high rate of false-negative results. At present, liquid based cytological screening technique ''Thin prep'' aided by Pap Net, an automated computer based visualization technique, seems to have increased the sensitivity of cytological screening. However, the efficiency of thin prep and Pap net are still under scrutiny.[5,6]

In case of a suspicious Pap smear or as an independent technique, colposcopy is performed. The major drawback of colposcopy is usually the lack of experience with a large enough patient population to become familiar with changes in premalignant and malignant conditions.[7] This often results in failure to recognize early disease conditions, and in errors like ''past pointing'', where the biopsied tissue does not come from the area of abnormality, but from an adjacent normal epithelium. Both Pap smear and colposcopy are prone to errors because of the subjective nature of the diagnosis.

Optical methods, which are fast, can be automated and can be made objective by statistical analysis, are therefore being considered as stand alone/complimentary technique for early detection. By forming standard calibration sets of pathologically certified samples in various stages of premalignancy/malignancy, and determining the statistical probability of how much a test sample matches with one of these sets, it is possible to have better diagnosis. Several groups[8–16] have studied fluorescence spectra of normal and malignant tissue to develop an optical pathology method for early detection of cancer. The optical method may also serve for monitoring effectiveness of therapy and early detection of recurrence without the need for biopsy.

For routine clinical usage, it is necessary to validate any new diagnostic method by different groups of investigators as well as for different ethnic classes. Optimization of the technique, validation by independent data sets and confirmation of spectral results by pathology, all will help in establishing the optical method as an acceptable technique. We have therefore carried out extensive fluorescence spectroscopic studies on tissue and tissue homogenate samples in cervical malignancy. The fluorescence spectra have been analyzed through multivariate analysis (principal component analysis) and curve resolution methods.

Our studies have shown that calibration data sets of fluorescence spectra with well-defined statistical parameters can be prepared for normal and malignant cervical tissue samples. Any test sample can then be matched against these standard sets to decide to which group the sample belongs, with good specificity and sensitivity.

Material and methods

Sample collection and handling

Normal (hysterectomy) and malignant cervical tissue samples were obtained from 62 subjects attending department of obstetrics and gynecology, Kasturba hospital, Manipal. The details of the patient population studied are shown in Table I. After biopsy or surgical resection the tissue specimens were rinsed, placed in ice cold physiological saline (pH = 7.4) and spectroscopic measurements were done immediately. Immediately adjacent part of the biopsy/surgical sample was fixed in 10% neutral buffered formalin and subjected to histopathology. Whenever necessary, the tissue samples were snap frozen in liquid nitrogen and stored at −80°C for later analysis. We have verified that no noticeable changes take place in spectra for such samples when compared with fresh samples.

Tissue homogenates were prepared by homogenizing 50 mg of fresh wet tissue in 200 μl of 10 mM Tris-EDTA buffer (pH 7.4) in a homogenizer (IKA-WERKE GMBH & Co. Germany Ultra Turrax T8) for 5 min. The homogenate was centrifuged and supernatant was collected. Twenty microliters of a suitably diluted supernatant was injected into an high performance liquid chromatography laser induced fluorescence (HPLC) system to separate the component proteins.

HPLC-LIF – tissue homogenate

The component proteins of the tissue homogenate were separated in a HP1100 HPLC system, using narrow-bore Vydac biphenyl column (Model 219TP52). The details of this set up are discussed elsewhere.[17] The effluent was passed through a quartz capillary flow cell (75 μm id, 300 μm od) where it was illuminated with a focused 257 nm beam from a frequency-doubled Argon ion laser (Coherent Innova Model FreD 90C). The fluorescence was collected at 90° on 1 side and measured using a JY - DH10 double slit

***Correspondence to:** Senior Scientist, Center for Laser Spectroscopy, Manipal Academy of Higher Education, Manipal. Karnataka, India 576104. Fax: +91-820-2571919. E-mail: sbkartha@hotmail.com or p-chidu@yahoo.com
Received 8 June 2005; Accepted 23 November 2005
DOI 10.1002/ijc.21825
Published online 31 January 2006 in Wiley InterScience (www.interscience.wiley.com).

TABLE I – SUMMARY OF PATIENT POPULATION STUDIED FOR FLUORESCENCE SPECTROSCOPY TECHNIQUE

	Number of subjects studied	Number of sites studied	Mean age in years ± SD
Normal	16	060	38 ± 6
FIGO stage III cancer	42	143	52 ± 8
Carcinoma *in situ*	04	015	32 ± 5

monochromator, Photo multiplier (Hamamatsu R750) and lock-in amplifier (EG&G Model No DSP 7265). Simultaneously the fluorescence spectra of eluted proteins were also recorded from the opposite side using a Spectra Pro 150 spectrograph coupled to a Princeton CCD (Roper Scientific, model RTE/CCD-128-HB).

Tissue fluorescence spectroscopy

Tissue samples were excited with an Nd-YAG- MOPO-FDO laser system (Spectra Physics Laser, USA, model PRO 230). Fluorescence spectra were recorded on an Acton (Spectra-Pro 150) spectrometer (slit width 200 μm, band pass 2.0 nm) equipped with a 300 g/mm grating, blazed for 300 nm. Dispersed spectra were accumulated with an Andor ICCD (Andor Technology, Northern Ireland DH-501-25F-01), gated with an SRS DG 535 delay generator. The DG 535 was triggered with the Q-Switch Advance signal from the laser. The details of the set up are discussed elsewhere.[18]

Each tissue specimen was mounted on a quartz plate and kept moist with the physiologic saline throughout the experiment. A conventional fiber optic probe was used to deliver the laser light and to collect the fluorescence. The probe consists of a 7-fiber assembly, with a central fiber to deliver the laser light and the surrounding 6 fibers to collect the fluorescence. The individual fibers (Thorlabs FG 200-UEP Fiber type) were 240 μm diameter with numerical aperture of 0.25. Two to 5 sites were studied on each tissue sample at any given excitation wavelength. No spectral changes were observed for exposures of up to even 2 hr with the pulsed laser radiation, as had been reported by others also.[19] All spectra were recorded by accumulating 500 pulses, and thus took less than a minute at the 10 Hz repetition rate.

Spectral data processing

The fluorescence spectra were corrected for background by a multiple point polynomial fit to remove the background. The resultant spectra were analyzed by the method of principal component analysis (PCA) and curve resolution techniques using GRAMS 32 and PLS Plus/IQ programs (Galactic Industries corporation, USA). Trial runs of PCA showed that 5 factors contribute to more than 98% of the total variance of the set of 218 spectra, and therefore, only 6 factors were used in all further spectral analysis.

PCA was done by 2 different approaches. In the first approach, the 218 spectra from normal, malignant and blind data were combined together and PCA was done with 6 factors (Principal Components), and their scores for each sample were evaluated. The scores were then used for discrimination between the normal and malignant tissue types. In the second method, 20 randomly selected spectra of pathologically certified normal/ malignant samples were used to form calibration sets. All spectra (including the members of the calibration set) were then matched (members of the calibration set retrospectively by rotating out one at a time and others prospectively) with the calibration sets to see to which set they belong. The second method obviously will be a better choice for situations where different stages have to be identified like CIN I, CIN II, *etc*. Comparison with calibration sets of each class can be then done for better diagnosis.

Spectra were also resolved into component bands by standard curve resolution techniques[20] to identify variations in fluorescence between normal and malignant samples, arising from changes in tissue components. Intensity ratio changes of pairs of resolved peaks were also tested for discrimination purposes.

Results

A total of about 1,000 spectra were measured on tissue specimens taken from 62 subjects with varying cervical pathology (16 Normal, 4 carcinoma *in situ* and 42 cancerous) at 4 excitation wavelengths, 275, 325, 375 and 425 nm. Figure 1 shows typical fluorescence spectra of normal and malignant cervical tissue on excitation at the earlier mentioned wave lengths. Since 325 nm excitation showed maximum difference between normal and malignant samples, excitation at 305–335 nm (at 10 nm intervals) was studied and again 325 nm excitation was found to be optimum. For a given pathologically certified normal or malignant sample, site-to-site variations were found to be only nominal as shown in Figure 2.

There are several statistical parameters like scores of factors, spectral residuals and Mahalanobis Distance[21,22] available for decision-making in PCA. As already mentioned, in the present work, 5 factors contributed to more than 98% of the total variance in the spectrum and the contributions of these factors to each spectrum give the scores for that spectrum. Samples belonging to a given class will have score values very close to each other, at least for the major factors. A scatter plot of the scores will thus serve as indicator of the sample type. The mean value and standard deviation of the scores of the calibration sets can then be used for decision-making.

When the scores of the significant factors for any spectrum are known the spectrum can be simulated and the spectral residual given by $R_s = \Sigma_i^p = {}_I(S_o^i - S_s^i)^2$ can be calculated as the sum of the squares of the differences between observed and simulated intensities across the p spectral points. Obviously, if the spectrum of a sample does not belong to a particular class, the spectral residual for that sample will be very high. Once again, the mean value and standard deviation of the spectral residuals of the calibration set can be used as statistical parameters for deciding whether a test sample belongs to that class or not.

The Mahalanobis Distance, a well-known statistical parameter, is defined for the present system by the equation $D^2 = (\mathbf{S}_{un})\ \mathbf{M}^{-1}\ (\mathbf{S}_{un})^1$ where $\mathbf{S}_{un}$ is the vector of scores and sum of squared spectral residual for a given unknown sample. $\mathbf{M}$ is the Mahalanobis matrix, given by $\mathbf{M} = \mathbf{S}^1\mathbf{S}/\ (n-1)$ where $\mathbf{S}$ is the n by f matrix of the standard calibration set of n standards, and f, their respective scores.

In the first method of PCA, all the 218 spectra obtained with 325 nm excitation were combined together, and the scores were evaluated with 6 factors. Figure 3 shows the scatter plot of the scores for factor 1 (contribution to spectral variance 68%) against sample number. In this plot, spectrum numbers 1–40 are from pathologically certified normal, and 41–75 from similar FIGO stage III cancer tissue specimens. The rest are test samples where the histopathology results were obtained after the spectroscopy analysis.

It is evident that for pathologically certified normal and malignant samples there is complete separation as clusters for scores of factor 1, indicating 100% sensitivity and specificity as shown on the left panel of the Figure 3. The results for the ''blind'' test samples are shown on the right panel of the figure. In the blind set all malignant stage IIIB tissue spectra have scores of that class except 5 spectra coming from 3 specimens indicated in boxes, which come in the range of normal category. The reasons for this are discussed later. No normal tissue specimens showed any overlapping with the scores of the malignant samples.

For the second method of PCA, in the present study, we have reasonably large number of samples for normal and stage III malignancy only. These 2 groups were therefore used to form calibration sets of 20 randomly selected spectra of each class and all samples were matched against these 2 sets. The results are shown

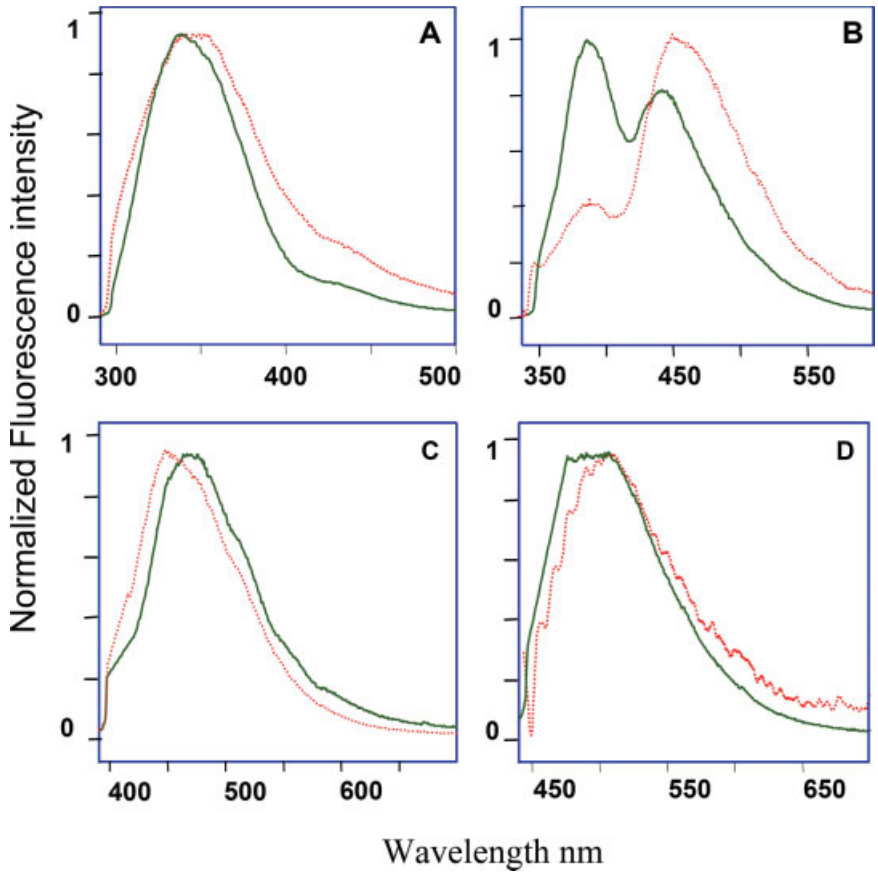

FIGURE 1 – Typical fluorescence spectra of normal and malignant cervical tissue samples at 4 excitation wave lengths: (*a*) 275; (*b*) 325; (*c*) 375 nm; (*d*) 425 nm. All spectra normalized to Peak intensity = 1. (——) Normal; (- - - -) Malignant.

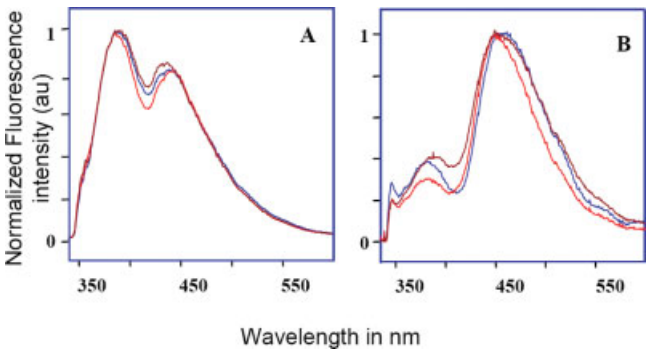

FIGURE 2 – Fluorescence spectra measured at different sites of pathologically certified Normal (*a*) and Malignant (*b*) tissue samples at 325 nm excitation.

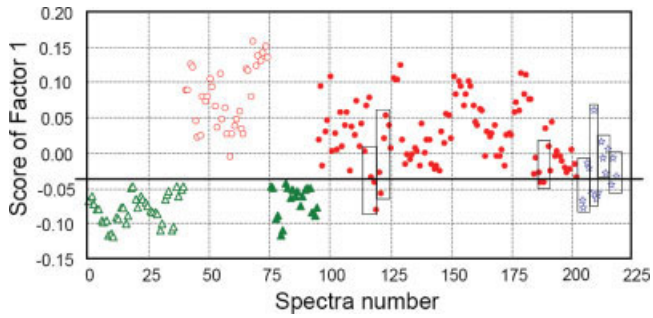

FIGURE 3 – Scatter plot of scores of factor 1 for 218 spectra. 1–40, Normal; 41–75, Malignant. On the right side, all spectra in any 1 box correspond to different sites on 1 sample. (Hollow triangles) pathologically certified Normal; (Hollow circles) pathologically certified Malignant; (Filled triangles) test samples – Normal; (Filled Circles) test samples – Malignant; (Hollow stars) CIS.

in Table II. Here, all the 218 spectra were matched against a calibration set of 20 spectra selected randomly from the pathologically certified normal sample spectra. The scores, spectral residuals, and Mahalanobis distances were used as parameters for matching. If a test sample matches in all 3 parameters, the range of values for the calibration set is classified as ''PASSED,'' otherwise as ''FAILED''.

It is well recognized that the total fluorescence of tissue arises from several biochemical species.[23] Generally the total fluorescence is assigned as arising from proteins with aromatic amino acids, collagen, NADH, flavins *etc*. Few attempts[24,25] have been made for separating the total fluorescence into those of individual components. We have studied this problem through curve resolution.

The fluorescence spectra for excitation at 275, 325 and 375 nm are quite asymmetric on a wavenumber scale and also shows weak shoulders, indicating more than 1 band in each case. For 275 nm, where protein fluorescence is dominant, curve fitting gave a strong peak at 345 nm with several weak peaks at shorter wavelengths. Also a medium intensity band was seen at around 390 nm. These bands have to come from different proteins (345 and below) and some collagen (390 nm) though collagen has only weak absorption at 275 nm. Similarly, 375 nm excitation gives 2 peaks for malignant tissue, 1 around 440 nm (bound NADH) and the other around 470 nm (free NADH). Excitation at 425 nm on the other hand gives only 1 peak at 500 nm for both normal and malignant samples and this can be from flavins. Figure 4 shows the curve fitting for 325 nm excitation. This shows the presence of about 4 bands so that it cannot be simply assigned to collagen and NADH (Free/Bound). However, the stronger peaks in these spectra correspond

TABLE II – MATCH/MISMATCH TEST BY PCA WITH CALIBRATION SET OF 20 RANDOMLY SELECTED, PATHOLOGICALLY CERTIFIED NORMAL TISSUE SPECTRA

	Match	Mahalanobis distance	Limit test[1]	Spectral residual
Spectra 1	Yes	0.20525	PASS (PPP)	0.36076
Spectra 2	Yes	0.69301	PASS (PPP)	0.95297
Spectra 3–40	Yes	–	PASS (PPP)	–
Spectra 41	No	28.88197	FAIL (FFF)	19.31267
Spectra 42	No	25.74399	FAIL (FFF)	17.31778
Spectra 43–75	No	–	FAIL (FFF)	–
Spectra 76	Yes	1.20861	PASS (PPP)	1.27771
Spectra 77	Yes	2.78025	PASS (P?P)	2.35817
Spectra 78–95	Yes	–	PASS (PPP)	–
Spectra 96	No	3.72024	FAIL (F?F)	2.99056
Spectra 97–203	No	–	–	–
Spectra 109[2]	Yes	1.76363	PASS (PPP)	1.61630
Spectra 118[2]	Yes	1.45786	PASS (PPP)	1.44354
Spectra 119[2]	Yes	0.78751	PASS (PPP)	0.90153
Spectra 120[2]	Yes	0.57438	PASS (PPP)	0.11071
Spectra 122[2]	Yes	0.56065	PASS (PPP)	0.51257
Spectra 192[2]	Yes	2.25837	PASS (PPP)	2.01522

Spectra 1–40 are pathologically classified as normal; spectra 41–75 pathologically classified as malignant; 76–95 test-normal sample; 96–203 test-malignant spectra of visually aided biopsy samples; 204–218 are spectra from carcinoma *in situ* samples.

[1]PPP – Mahalanobis distance, spectral residual, score.–[2]Abnormal blind samples of Figure 3. See text for details.

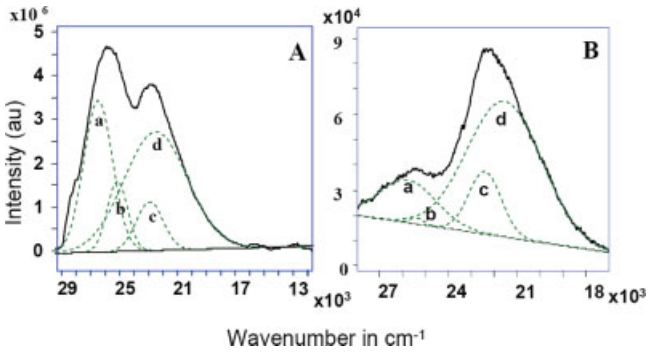

FIGURE 4 – Typical curve-fitted spectrum at 325 nm Excitation. (*a*) Normal; (*b*) Malignant. (——) Observed spectrum; (- - - -) fitted curves.

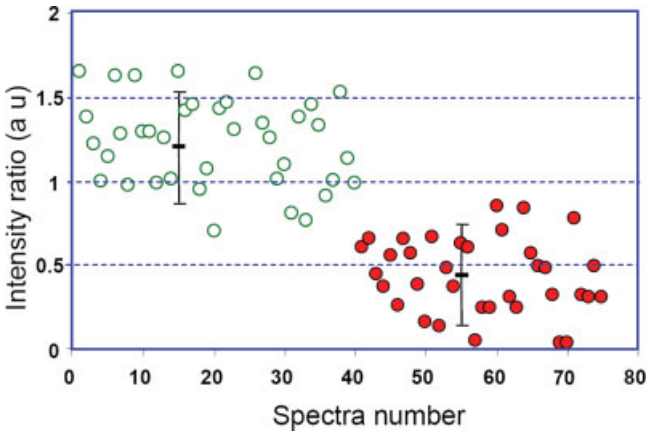

FIGURE 5 – Intensity ratio of resolved peaks (*a*) and (*d*) of Figure 4. (Hollow circles) pathologically certified normal tissue spectra; (Filled circles) pathologically certified malignant tissue spectra.

to collagen and NADH.[26] The intensity ratios of these peaks for normal and malignant samples are plotted in Figure 5. It can be seen that there is substantial difference in the ratio of concentration of collagen to NADH in malignancy, as shown by earlier workers also.[25]

It is well known that Hemoglobin has strong absorption in this region, peaking at around 420 nm. The dip in the fluorescence spectrum can thus be attributed to this Hb absorption. However, while this is likely for *in vivo* observations, in our studies there is very little chance for Hb absorption for the following reason. Since all samples were collected in saline and removed from this medium before taking spectrum, any blood originally present will mostly be removed from the sample. Also if the dip was from Hb absorption, it should have been more in malignant samples due to possible increase in Hb content because of angiogenesis. Further, time-delayed spectroscopy[18] shows that the fluorescence in this region comes from 2 major bands with entirely different time evolution.

The presence of several molecular species under a general category like proteins becomes evident from our results on tissue homogenates. Figure 6 shows the chromatograms of tissue homogenates from normal and malignant tissues. These were recorded by detecting the fluorescence at 340 nm ''on-the-fly''[17]; and show the concentrations of different proteins in the homogenate. It can be seen that the total protein spectrum observed at 275 nm (Fig. 1*a*) excitation comes from overlapping spectra of several proteins. It is clear that there are noticeable differences in the spectra, a fact which is not obvious from the total spectrum, because of the overlapping.

Discussion

Immunological, biochemical and other techniques like fluorescence imaging are in use for identification and classification of various stages of a cancer. However, these methods are time consuming and are often expensive. Recently fluorescence based analysis of cellular constituents have been investigated.[27] In the present study, we have analyzed laser-induced fluorescence of cervical cancer tissues compared to its normal counterpart. We have further refined the data using statistical analysis and checked test samples to evaluate its usefulness in diagnosis. Our major findings are (*i*) excitation at 325 nm gives better discrimination between normal and malignant tissues. (*ii*) Variation in fluorescence spectra at different sites of the tumor or normal tissue specimen is minimal when pathologically certified biopsy samples are studied. Site-to-site variations may be observed in malignant tissue specimens taken through visual examination. (*iii*) Matching of a test sample to calibration sets can provide objective, reliable diagnosis.

In many earlier fluorescence and Raman techniques[28,29] when a number of spectra are recorded from different sites of 1 tissue

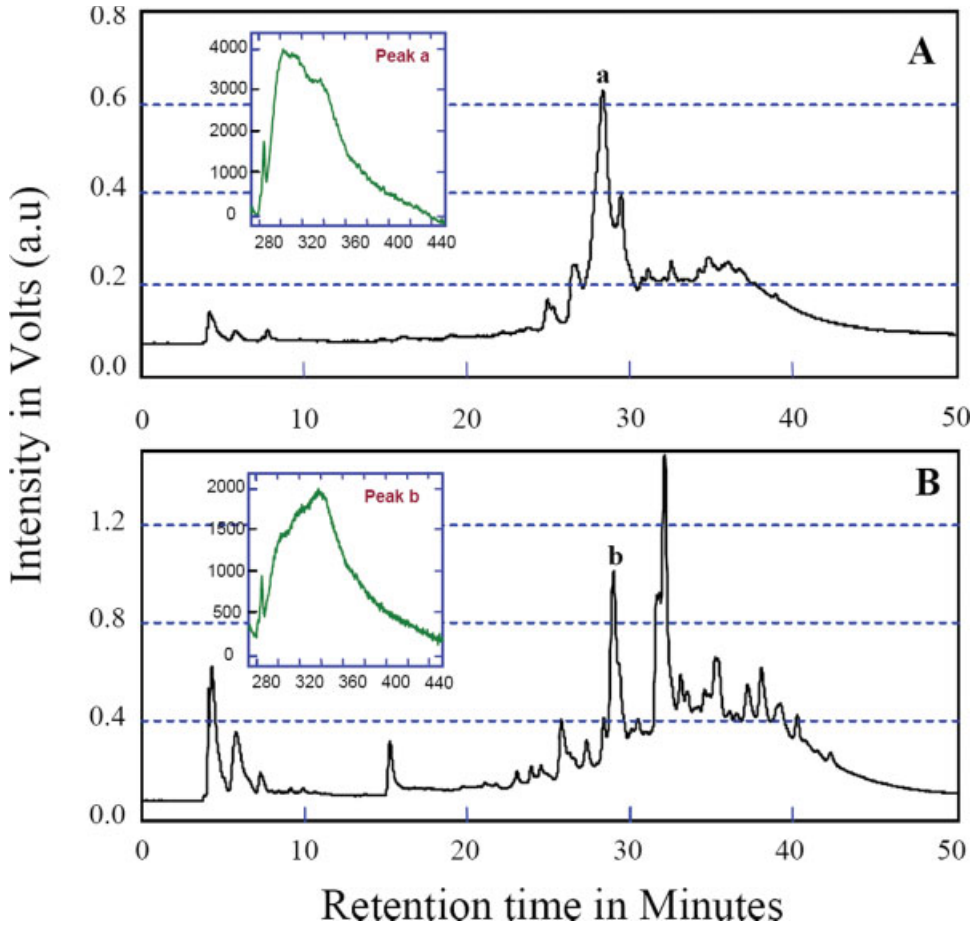

FIGURE 6 – HPLC peaks from tissue homogenates. (*a*) Normal. (*b*) Malignant. Vydac Narrow Bore Biphenyl (Model 219TP52) Column. Gradient – 80% H_2O, 20% Acetonitrile at time = 0 min. And 20% H_2O, 80% Acetonitrile at time = 60 min. The fluorescence spectra of 2 peaks 'a' and 'b' which are eluting at the same time are shown as insets in the corresponding figure.

sample, the mean of these is taken as representative of that sample for further data processing and evaluation. In the present work, the 218 spectra obtained from 62 samples are treated as independent data. This, we believe, is a better approach for the following reasons. First, in epithelial cancers, like carcinoma of the cervical mucosa, (before it has penetrated the underlying tissue), often a tissue specimen can have normal and anaplastic regions adjacent to each other.[30] The pathologist examines several sites on a biopsy sample and even if 1 site shows as abnormal, sample is considered as abnormal. Secondly, for *in vivo* applications in screening, surgical boundary demarcation and optically guided biopsy it is necessary to identify the exact site where malignancy begins or terminates. The variations in the spectra from site to site will be the deciding factor in these situations and they have to be treated independently. Thirdly, in epithelial cancers the abnormal proliferation starts near the basal lamina and advances into the epithelial region, and eventually in the invasive stage penetrates in the connective tissue region. We have shown[31] by Raman spectroscopy that in biopsied tissue samples of oral cancer, the sub-epithelial region showed very similar spectra for normal and malignant samples, and only the epithelial spectra discriminated between the 2 very well. This indicates that unless one is sure which region (epithelial, sub-epithelial or connective tissue) one is looking at in a malignant sample there can be both normal and malignant types of spectra from adjacent sections of the same sample. It is thus clear that when there is no *a priory* information available for a sample it is necessary to examine many sites on the sample and treat each site as different.

In Figure 3, we have shown the scores for all the spectra. For pathologically certified normal and malignant samples there is complete separation between the clusters for the 2 classes of samples indicating 100% sensitivity and specificity. In the results for the test samples shown on the right panel of the figure, an overlapping with the normal class can be seen in 5 spectra from the malignant test samples indicated in the boxes. This is due to the presence of normal tissue sections in the biopsy and it has been further confirmed with the histopathological analysis. This possibility of normal tissue contamination in biopsy sections obtained through visual identification is very important when analyzing the precancerous stages, where the number of transformed cells can be quite small. Our results on precancerous tissue, shown in the extreme right panel of Figure 3, indicate a distribution of spectral scores in both normal and malignant categories. From these results it is evident that a sample should be screened at several sites, and each site should be treated independently. The sample should be categorized as malignant even if a single site shows malignant spectral features. This is further supported by the result that there is absolutely no overlapping for the normal specimens. The normal tissue contamination also raises concern over the routine biopsy procedure aided only by visual techniques. In this case, we feel that a biopsy guided by fluorescence spectroscopy can yield more accurate diagnosis. Further, the technique is also helpful in demarkation of the surgical area during the tumor removal. It is clear that any spectral studies either *in vivo* or *in vitro* (biopsy) should cover as many sites as possible during a routine screening to minimize the chances of a premalignant/malignant condition being classified as normal. The fluorescence technique can compliment visual judgment for biopsy even in inexperienced hands.

It may be possible that if there are many groups of data set (*e.g.* HPV infection, inflammation, CIN I, CIN II *etc*) the scores for 1 or more factors may still group in different clusters, and a correct diagnosis may be possible when all the data are processed together. However, it is more likely that the scores may overlap because of slowly varying spectral characteristics and may cover a

wide range. Clear discrimination may then become difficult using only scores of factors.

When calibration sets are available for the different stages (*e.g.* pathologically classified sets of CINI, CINII *etc.*) of the disease, a PCA can be done with each set. Any new sample can then be matched against each calibration set and a more reliable classification may be achieved by identifying the set to which the sample matches best. It is seen from Table II, that all normal spectra (including the pathologically certified, but not included in the calibration set, as well as test spectra) pass the match/mismatch test. Out of 143 spectra from 42 malignant samples, 6 spectra pass the limit test as normal. These correspond to those that fell into the factor 1 score region of normal samples in Figure 3. The other spectra from these tissue samples classified as ''fail,'' that is, malignant. Since a sample has to be considered as malignant even if 1 site turns out to be malignant, this type of matching leads to 100% sensitivity and specificity!

The pass/fail test with a calibration set of 20 randomly selected spectra from the malignant group gave all normal as ''fail'' giving a specificity of 100%. Out of 143 malignant sample spectra, 113 classified as ''pass,'' and 20 classified as ''possible,'' meaning they match 2 out of the 3 parameters very well and the third parameter to some extent. Since the ''possible'' failed to match the normal calibration set, they can be classified as malignant. Ten samples failed to match with the malignant set. Out of the 10, 6 are those mentioned earlier which matched with the normal set. The remaining misclassification may arise from several reasons like the sites not corresponding to Stage III B. This is supported by the fact that these samples also failed to match the normal calibration set.

The results of the curve resolution studies, and ratio of intensity plots show that this method could also possibly be used for discrimination between normal and stage III malignancies. For example, the intensity ratios of the resolved bands are plotted against sample number in Figure 5. Out of the possible combinations of bands, only those common to both normal and malignant tissues are shown in this figure. Earlier workers have generally assigned the 2 observed broad peaks at about 390 and 450 nm to collagen and NADH, respectively. Changes in relative intensities have been attributed to thickening of epithelial layer, loss of collagen and increase in NADH level in malignancy. However, curve resolution studies show that there are 4 peaks in this region (Fig. 4) indicating other components in addition to collagen and NADH. Also the changes in peak positions and intensities of these bands between normal and malignant samples show that they exist in very different environmental situations, leading to different radiative and nonradiative processes. Figure 5 (peak a: peak d) showing the collagen: NADH ratio seems to give better discrimination between normal and Stage III samples compared to ratio of other peaks. However, in general, the discrimination here is inferior to that observed with PCA.

We have carried out similar PCA studies with the fluorescence spectra excited by 275 nm also since the spectra showed some differences between normal and malignant samples. However, the sensitivity and specificity were not as good in this case as for 325 nm excitation.

The high performance liquid chromatography laser induced fluorescence (HPLC-LIF) result of tissue homogenates shows the differential expression of several proteins in malignancy, a result of increased rate of cell proliferation and metabolism. The interesting result here is that even the proteins eluting at the same time (peaks a and b of Fig. 6) seem to be different in structure as seen from their fluorescence spectra shown as inset in each case. This may be because of presence of an altered protein in malignancy, and could serve as a possible tumor marker. The sensitivity of HPLC-LIF is very high and we have shown that our system can detect sub-femtomole quantities as of now, and this sensitivity can further be increased 2–3 orders of magnitude if required.[17] It is thus quite likely that this method of protein profile analysis can be used with great advantage for early detection and staging of cervical cancer with tissue homogenate, cell lysates (Pap smear) and cervical wash samples.

In conclusion, we have shown that PCA based multivariate analysis with different calibration sets corresponding to different stages of disease can be used with higher sensitivity and specificity for predicting a new sample. Also spectral results closely match the pathology results even when there is no prior information, indicating fluorescence spectroscopy method can be used for successful location of biopsy sites as a stand-alone technique or complementary method to colposcopy. Curve resolution studies have indicated the contribution of fluorescence species other than collagen and NADH at 325 nm excitation. In the same manner, spectra of chromatographically separated proteins from tissue homogenates have been shown to have very different spectra, even though the tissue fluorescence showed more or less a single fluorescence peak in this region. It should be emphasized that the spectroscopic evaluation of samples takes very little time [few minutes] and could provide an objective, fast method for rapid screening and diagnosis in cervical cancer.

Acknowledgements

This work was done under the Department Of Atomic Energy/ Board of Research in Nuclear Science Project No. 98/34/14/BRNS Cell/1090, and Department of Science and Technology Project No. SP/S2/L01/98, Government of India.

References

1. Jamal A, Thomas A, Murray T, Thum M. Cancer statistics, 2002. CA Cancer J Clin 2002;52:23–4.
2. Notani NP. Global variation in cancer incidence and mortality. Curr Sci 2001;81:465–74.
3. Fahey MT, Irwig L, Macaskill P. Meta-analysis of Pap test accuracy. Am J Epidemiol 1995;141:680–4.
4. Koss LG. The Papanicolaou test for cervical cancer detection. A triumph and a tragedy. JAMA 1989;261:737–43.
5. Mudu P, Migliore G, Alderisio M, Morosini P, Douglas G, Navone R, Montanari G, Bonito DL, Vitali A, Moretti D, Giovagnoli MR, Fulciniti F, et al. Papnet-assisted cytological diagnosis intensifies the already marked variability among cytological laboratories. Eur J Gynaecol Oncol 2002; 23:211–5.
6. Schorge JO, Hossein SM, Hynan L, Ashfaq R. ThinPrep detection of cervical and endometrial adenocarcinoma: a retrospective cohort study. Cancer 2002;96:338–43.
7. Mitchell MF. Accuracy of colposcopy. Consult Obst Gynecol 1994;6: 70–3.
8. Andres FZ, Utzinger U, Durkin A, Fuchs H, Gillenwater A, Jacob R, Kemp B, Fan J, Richards-Kortum R. Fluorescence excitation emission matrices of human tissue: a system for *in vivo* measurement and method of data analysis. Appl Spectrosc 1999;53:302–11.
9. Leiner MJ, Schaur RJ, Desoye G, Wolfbeis OS. Fluorescence topography in biology. III: characteristic deviations of tryptophan fluorescence in sera of patients with gynecological tumors. Clin Chem 1986;32:1974–8.
10. Hubmann MR, Leiner MJ, Schaur RJ. Ultraviolet fluorescence of human sera: I. Sources of characteristic differences in the ultraviolet fluorescence spectra of sera from normal and cancer-bearing humans. Clin Chem 1990;36:1880–3.
11. Heintzelman DL, Utzinger U, Fuchs H, Zuluaga A, Gossage K, Gillenwater AM, Jacob R, Kemp B, Richards-Kortum R. Optimal excitation wavelengths for in vivo detection of oral neoplasia using fluorescence spectroscopy. Photochem Photobiol 2000;72:103–13.
12. Brookner CK, Utzinger U, Staerkel G, Richards-Kortum R, Mitchell MF. Cervical fluorescence of normal women. Lasers Surg Med 1999;24:29–37.
13. Grossman N, Ilovitz E, Chaims O, Salman A, Jagannathan R, Mark S, Cohen B, Gopas J, Mordechai S. Fluorescence spectroscopy for detection of malignancy: H-ras overexpressing fibroblasts as a model. J Biochem Biophys Methods 2001;50:53–63.
14. Agrawal A, Utzinger U, Brookner C, Pitris C, Mitchell MF, Richards-Kortum R. Fluorescence spectroscopy of the cervix: influence of acetic acid, cervical mucus, and vaginal medications. Lasers Surg Med 1999;25:237–49.

15. Ramanujam N, Richards-Kortum R, Thomsen SL, Mahadevan A, Mitchell MF, Chance B. Low temperature fluorescence imaging of freeze-trapped human cervical tissues. Opt Express 2001;8:336–43.
16. Ramanujam N, Mitchell MF, Mahadevan A, Warren S, Thomson S, Silva E, Richards-Kortum R. *In vivo* diagnosis of cervical intraepithelial neoplasia using 337-nm-excited laser-induced fluorescence. Proc Natl Acad USA 1994;91:10193–7.
17. Venkatakrishna K, Kartha VB, Keerthilatha MP, Muralikrishna C, Ravikiran O, Kurian J, Alexander M, Ullas G. HPLC-LIF for early detection of oral cancer. Curr Sci 2003;84:551–7.
18. Manjunath BK, Kurein J, Rao L, Krishna CM, Chidananda MS, Venkatakrishna K, Kartha VB. Autofluorescence of oral tissue for optical pathology in oral malignancy. J Photochem Photobiol 2004;73:49–58.
19. Palmer GM, Marshek CL, Vrotsos KM, Ramanujam N. Optimal methods for fluorescence and diffuse reflectance measurements of tissue biopsy samples. Lasers Surg Med 2002;30:191–200.
20. Percampus HH. Evaluation of UV-VIS spectral bands, UV-VIS spectroscopy and its application. New York: Springer-Verlag, 1992. 220–8.
21. Mark HL. Normalized distances for qualitative near-infrared reflectance analysis. Anal Chem 1986;58:379–84.
22. Mark H, Tunnel D. Qualitative near infrared reflectance analysis using Mahalanobis distance. Anal Chem 1985;57:1449–54.
23. Wagnieres GA, Star WM, Wilson BC. In vivo fluorescence spectroscopy and imaging for oncological applications. Photochem Photobiol 1998;68:603–32.
24. Georgakoudi I, Jacobson BC, Muller MG, Sheets EE, Badizadegan K, Carr-Locke DL, Crum CP, Boone CW, Dasari RR, Van Dam J, Feld MS. NAD(P)H and collagen as in vivo quantitative fluorescent biomarkers of epithelial precancerous changes. Cancer Res 2002;62:682–7.
25. Drezek R, Sokolov K, Utzinger U, Boiko I, Malpica A, Follen M, Richards-Kortum R. Understanding the contributions of NADH and collagen to cervical tissue fluorescence spectra: modeling, measurements, and implications. J Biomed Opt 2001;6:385–96.
26. Muller MG, Valdez TA, Georgakoudi I, Backman V, Fuentes C, Kabani S, Laver N, Wang Z, Boone CW, Dasari RR, Shapshay SM, Feld MS. Spectroscopic detection and evaluation of morphologic and biochemical changes in early human oral carcinoma. Cancer 2003;97:1681–92.
27. Altiok S. Molecular markers in cervical cytology. Clin Lab Med 2003;23:709–28.
28. Ramanujam N, Mitchell MF, Mahadevan-Jansen A, Thomsen SL, Staerkel G, Malpica A, Wright T, Atkinson N, Richards-Kortum R. Cervical precancer detection using a multivariate statistical algorithm based on laser-induced fluorescence spectra at multiple excitation wavelengths. Photochem Photobiol 1996;64:720–35.
29. Utzinger U, Brewer M, Silva E, Gershenson D, Blast RC, Jr., Follen M, Richards-Kortum R. Reflectance spectroscopy for in vivo characterization of ovarian tissue. Lasers Surg Med 2001;28:56–66.
30. Robins SL, Kumar L, eds. Basic pathology, 4th ed. Philadelphia: WB Saunders, 1987.189p
31. Krishna CM, Sockalingum GD, Kurien J, Rao L, Venteo L, Pluot M, Manfait M, Kartha VB. Micro-Raman spectroscopy for optical pathology of oral squamous cell carcinoma. Appl Spectrosc 2004;58:1128–35.